Seismic Hazard Estimation Based on Non-Poisson Earthquake Occurrences*

By

Hiroyuki KAMEDA** and Hideki TAKAGI***

(Received March 30, 1981)

Abstract

A non-Poisson earthquake occurrence model for seismic hazard estimation is developed to account for the periodicity and the nonstationarity in seismic activities. The model consists of a renewal process model for major fault systems and a nonstationary Poisson-type model for secondary seismic sources, the latter being dominated by the former. The model is identified on the basis of the historical earthquake data for the Kinki District in the western part of Japan, containing the Kyoto-Osaka-Kobe metropolitan area.

A simulation model for seismic hazard estimations (ground acceleration and velocity are dealt with) is then developed by combining the non-Poisson earthquake occurrence model and probabilistic attenuation rules. On the basis of the results of the simulation, the significance of the periodicity and the nonstationarity of seismic activities in assessing the seismic risk is discussed.

1. Introduction

Seismic hazard estimation constitutes a basis for seismic risk and seismic design decision for engineering structures and facilities. Probabilistic methods are commonly used for this purpose in order to account for the uncertainties of location, magnitude, and time of occurrence of destructive earthquakes. Many works have been published on probabilistic estimation, of earthquake hazards for Japan[7,10,14,15,20], for the United States[3,4,6], as well as for other parts of the world. Hazard parameters include peak ground acceleration or velocity, response spectra, effective peak acceleration, etc. The probabilistic models in these studies are based on somewhat different ideas as to the type of seismic sources and attenuation rules, but they are all essentially based on Poisson-type earthquake occurrence models; i.e., stationary and independent random earthquake occurrences are assumed.

* This work was presented in the same form at the Review Meeting for the U.S.-Japan Cooperative Research on Seismic Risk Analysis and Its Application to Reliability-Based Design of Lifeline Systems, Honolulu, January 1981.

** Department of Transportation Engineering.

*** Nagoya Railways Co.

When we observe a limited seismic source area that will affect specific sites for engineering structures, there is no doubt that a correlation does exist between the occurrence of consecutive destructive earthquakes. This is a consequence of a widely recognized idea that after a major earthquake has occurred in a seismic region, a certain period must elapse for the accumulation of strain energy sufficient to cause the next earthquake. There is also evidence that the occurrence rate of destructive earthquakes in minor seismic sources varies with time, being controlled by those occurring in major fault systems dominating the seismo-tectonic activities of the area. This feature will result in nonstationarity and a cyclic variation of seismic activities.

Despite the correlation and nonstationary of earthquake occurrences as described above, a Poisson-type model is appropriate if the time span to be discussed is long enough for a complete cycle or two of major seismic activities of the area to be repeated, and the effects of correlation and nonstationarity are eliminated through time-averaging. However, the period of these seismic activities would usually be very long, say at least some hundreds of years, which is much longer than the time scale of normal human activities and required useful lives of ordinary engineering structures and facilities. Therefore, Poisson-type earthquake occurrence models that can answer only questions about long-term engineering problems will often fail to provide accurate information for relatively short-term problems. Short-term problems require clarification of the seismic risk for a certain future period starting from 'now'. Engineers want to know what will be the future risk with a knowledge of the previous destructive earthquake. This requires the introduction of an absolute time axis, instead of the relative time axis on which Poisson-type models are based.

In this view of the problem, Kameda and Ozaki[12] analyzed the historical earthquake data experienced in Kyoto, Japan, and pointed out that the mean earthquake occurrence rate increases with the interval between two successive earthquakes. Based on this, they applied a renewal process model to estimate the probability of future earthquake occurrence along the absolute time axis. Nishioka and Shah[17] proposed to use Markov chains for the earthquake occurrence, and applied them to Tokyo, demonstrating that the periodicity of earthquake occurrences can be reasonably considered.

These two works using certain non-Poisson models deal with estimation of earthquake occurrences observed at fixed sites. For a wider engineering use, it is desirable to develop more general models that can generate information on seismic risk for arbitrary sites within a certain semismic area, such as those dealt with the in above-mentioned works using Poisson-type models.

The objective of this study is to develop a probabilistic model for a seismic hazard estimation incorporating non-Poisson features of earthquake occurrences that will provide information on the future seismic risk along an absolute time axis. The earthquake occurrence model is developed as a combination of (1) a renewal process (R-model) for great earthquakes occuring along a major fault system, and (2) a nonstationary Poisson process model (N-model) for other destructive earthquakes located along secondary fault systems and minor seismic source areas. The time-variation of the occurrence rate for the N-model is dominated by the interval of the great earthquakes dealt with in the R-model.

For an illustrative application, a seismic area containing the Kyoto-Osaka-Kobe metropolitan area, called the Kinki District, a western part of Japan, is analyzed. Seismo-tectonic features of the area are examined, from which the R-model is developed for great earthquakes taking place along an off-shore plate boundary, and a system of N-models is identified for in-land seismic areas. Then a simulation model for a seismic hazard estimation is developed by combining the earthquake occurrence model and a probabilistic attenuation rule. The results of simulation are presented in various forms convenient for engineering applications, including mean numbers of earthquakes, contribution of each source area to a particular site, mean value and probability distribution of the maximum ground acceleration and the maximum ground velocity. In particular, the effect of periodicity and nonstationarity of earthquake occurrence on a seismic hazard estimation in comparison with Poisson-type models is discussed.

2. Non-Poisson Earthquake Occurrence Model

2.1 Seismicity and seismo-tectonic features of major fault systems and secondary sources based on the data for the Kinki District

Since the methodology developed herein is focused primarily on application to the Kinki District, the seismicity and the seismo-tectonic features of the area are discussed in relation to the modeling of its seismic occurrences.

Fig. 1 shows the location of the area, and the epicenters of historical earthquakes with an estimated magnitude* M no less than 6.0. The total of 74 earthquakes shown in Fig. 1 occurred within the past 1100 years ranging from 887 A.D. to 1972 A.D. Epicentral locations and magnitudes of old earthquakes have been estimated from descriptions on their damage[23]. The locations and magnitudes of these earthquakes are listed in Table A1 in Appendix A. In Fig. 1, the whole area has been

* Throughout this study, only earthquakes with $M \geqq 6.0$ will be dealt with. This range has been determined to eliminate non-hazardous earthquakes.

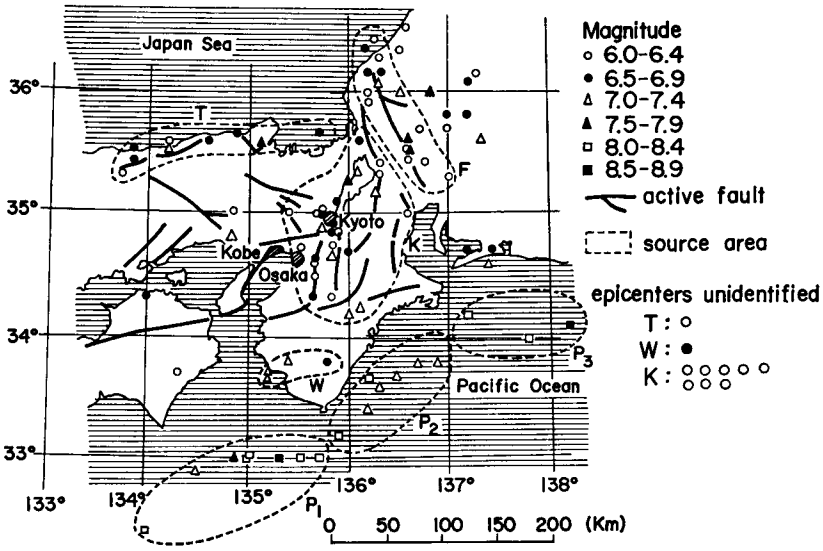

Fig. 1. Seismic Activities of the Kinki District.

divided into several source areas that will be used throughout this study. Seismic activities of the Kinki District may be summarized as follows.

First, it is pointed out that great earthquakes with M=8~8.6 take place with intervals of some 90~250 years in the off-shore seismic source P (subdivided into P_1, P_2 and P_3). Sometimes a pair of great earthquakes occur successively with such short intervals that they should be treated as highly correlated events. (See, for example, the pair of earthquakes occurring in source P on Dec. 23 and Dec. 24, 1854, and also those on Dec. 7, 1944 and Dec. 21, 1946.) The effect of these "twin-events" will also be incorporated in the earthquake occurrence model. During these great earthquakes, fault rupture takes place throughout the whole area of at least one of the fixed sources P_1, P_2, or P_3. These great earthquakes have been explained by seismologists in relation to the subduction of the Phillippine-Sea plate into the Asia plate. Accumulation and release of tectonic stresses along source P apparently dominate the seismic activities of the whole area, as described below.

Observe next the seismic activities in the other source areas located in in-land districts. Although the earthquakes occurring in the in-land sources are of magnitudes generally smaller than the great earthquakes in the off-shore source P, they have greater hazardous effects on the metropolitan area because of short epicentral distances. Fig. 2 shows the history of destructive earthquakes that occurred in sources P and K. For source P, only the great earthquakes with magnitudes no

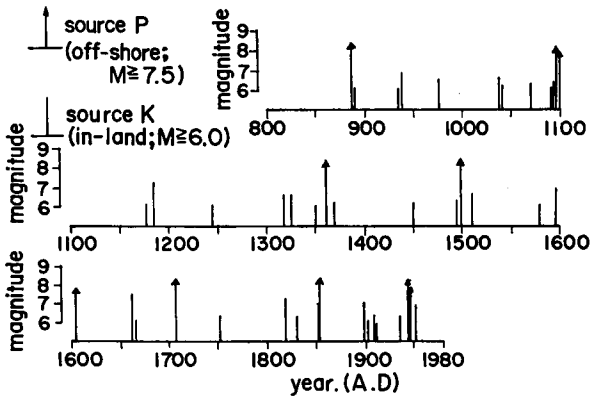

Fig. 2. History of Destructive Earthquakes in Sources P and K.

less than 7.5 are shown. It is observed that the occurrence of in-land earthquakes tend to cluster within time ranges of some 50 years before the occurrence of great off-shore earthquakes, and some 20 years thereafter. This aspect has been explained from a seismological viewpoint by Ozawa[18] in the following manner. The tectonic stress fields of the whole area in Fig. 1 are dominated primarily by the stress accumulation and release in source P, connected with the occurrence of great off-shore earthquakes. After the occurrence of a great off-shore earthquake which releases the stress of the whole area, a quiescent period lasts for some time. As tectonic stresses are accumulated, the in-land sources enter an active period, and in-land type destructive earthquakes continue to occur randomly both in time and location until the next great off-shore earthquake releases the stresses of the area. The in-land earthquakes immediately following the great off-shore earthquake should be considered as aftershocks in a wide sense.

From the foregoing discussion, the seismic activities of the Kinki District may be characterized by a periodic occurrence (with random intervals) of great off-shore earthquakes on the plate boundary, and a nonstationary random occurrence of in-land earthquakes whose occurrence rates vary with time, in accordance with the stress accumulation and release dominated by great off-shore earthquakes. The significance of incorporating the periodicity and the non-stationarity in engineering seismic risk analysis, which is the objective of this study, should be clear from the discussion in the previous chapter.

It will be of interest to examine if similar situations exist in the seismic activities of other areas. Ishibashi[11] pointed out possible interactions between great earthquakes occurrin on major fault systems on plate boundaries and those in in-land sources in eastern Japan. As many active seismic areas of the other parts

of the earth are located close to plate boundaries, it may be of value for engineering purposes to perform similar works on those areas through careful observation of earthquake histories.

2.2 Renewal process model (R-model) for major seismic fault systems

The occurrence of great off-shore earthquakes occurring in the P is modeled. A renewal process model with a probabilistic source migration is developed, after examining the stationarity, recurrence time distribution, and the source locations.

Stationarity of energy release.—The history of energy release in source P is shown in Fig. 3. The seismic energy E, released by an earthquake with a magnitude M, has been calculated from the following formula[23].

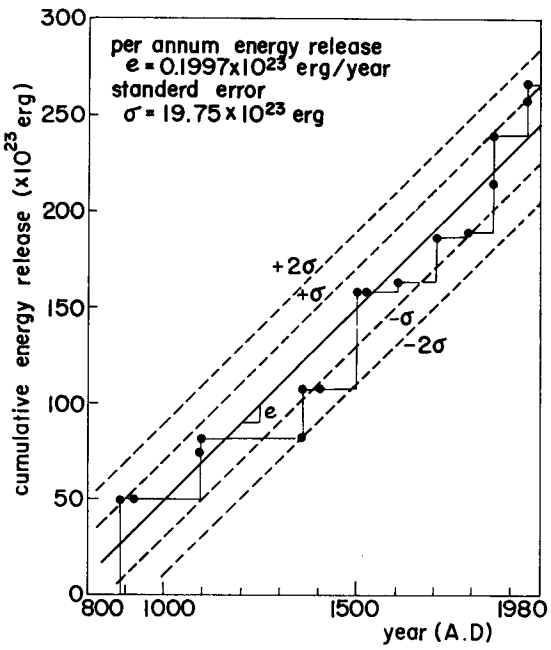

Fig. 3. History of Energy Release in the Source P (887A.D.–1980A.D.).

$$\log E = 11.8+1.5M \qquad \cdots\cdots(1)$$

It may be concluded from Fig. 3 that the energy release in source P is stationary.

Recurrence time distribution.—In Fig. 4, the cumulative probability of intervals (recurrence times) between great off-shore earthquakes is plotted on an exponential probability paper. Herein, the "twin-events" identified in Fig. 5 are counted as single events. From Fig. 4, it will be appropriate to model the recurrence time distribution with a shifted exponential distribution[1] with a lower bound

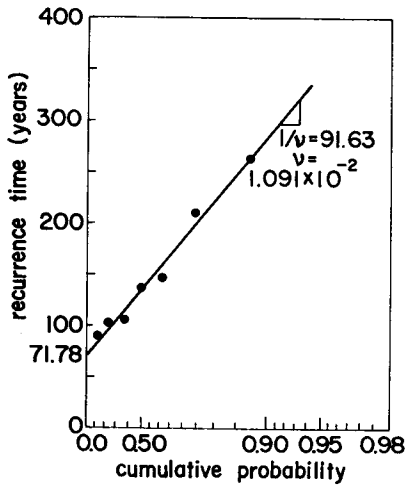

Fig. 4. Recurrence-Time Distribution for Great Off-Shore Earthquakes. (Source (P))

of $t_0=71.8$ years and a parameter of $\nu\times 1.0191\times 10^{-2}$ year^{-1}. Additionally, it is noted that there should be an upper bound on the recurrence time considering the periodic aspects of the phenomena. An upper bound of $t_u=270$ years will be used in this study.

From these arguments, the distribution function for the recurrence time T_r of great off-shore earthquakes is formulated as

$$F_{T_r}(t)=\begin{cases}1; & t>t_u\\ \dfrac{1-\exp\left[-\nu(t-t_0)\right]}{1-\exp\left[-\nu(t_u-t_0)\right]}; & t_0\leqq t\leqq t_u\\ 0; & t<t_0\end{cases} \qquad \cdots\cdots\cdots\cdots(2)$$

where $t_0=71.8$ years, $t_u=270$ years, and $\nu=1.091\times 10^{-2}$ year^{-1}.

The return period μ_{T_r} is obtained as

$$\mu_{T_r}=\int_{t_0}^{t_u} t\,dF_{T_r}(t)=\frac{(1+\nu t_0)-(1+\nu t_u)e^{-\nu(t_u-t_0)}}{\nu\left[1-e^{-\nu(t_u-t_0)}\right]}=137.7 \text{ years} \cdots\cdots\cdots(3)$$

By assuming a statistical independence between recurrence times, the occurrence model for great off-shore earthquakes in major fault systems using Eq. 2 constitutes a renewal process.

Magnitude distribution.—Considering that our attention is being confined to great off-shore earthquakes and that their actual magnitudes vary in a narrow range of 7.9~8.6, a uniform distribution in the range of 8.0~8.6 is assumed for

their magnitude distribution; i.e., its probability density function $f_M(m)$ takes the form

$$f_M(m) = \begin{cases} 0 \quad ; & m<8.0,\ m>8.6 \\ 1.667; & 8.0 \leqq m \leqq 8.6 \end{cases} \qquad \cdots\cdots\cdots\cdots\cdots\cdots (4)$$

Migration of sources.—Fig. 5 shows how the sources of great off-shore earthquakes have migrated from one to another in the source areas P_1, P_2, and P_3. The "twin events" are shown by double lines. Observe that source P_1 has been most active and that migration in twin events always terminates in source P_1, starting from one of the other two. A Markov chain is employed for the probabilistic model of the source migration which follows.

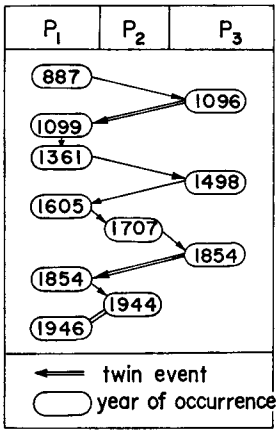

Fig. 5. Source Migration of Great Off-Shore Earthquakes.

(i) Source migrations are classified into independent migrations and twin-event migrations. The former take place in the renewal process characterized by Eq. (2), and the latter take place as the second of a twin event. The intervals between twin events which are actually in a range between one day and three years are neglected in the model.

(ii) An earthquake occurring in source P_j, $(j=1, 2, 3)$ in an independent migration will be accompanied by a twin-event migration with a probability p_{dj}, $(j=(1, 2, 3)$. The twin-event probability p_{dj} has been determined as

$$\{p_{dj}\} = \{0.0,\ 0.5,\ 0.667\} \qquad \cdots\cdots\cdots\cdots\cdots\cdots (5)$$

(iii) The probability of migration from source P_j to source P_j in an independent migration, denoted by s_{ij}, and that in a twin-event migration, denoted by

d_{ij}, are given, respectively, by the following transition probability matrices.

$$[s_{ij}] = \begin{bmatrix} 0.2 & 0.4 & 0.4 \\ 0.0 & 0.0 & 1.0 \\ 1.0 & 0.0 & 0.0 \end{bmatrix} \quad \cdots\cdots(6)$$

$$[d_{ij}] = \begin{bmatrix} 1.0 & 0.0 & 0.0 \\ 1.0 & 0.0 & 0.0 \\ 1.0 & 0.0 & 0.0 \end{bmatrix} \quad \cdots\cdots(7)$$

2.3 Nonstationary occurrence model (N-model) for secondary seismic sources

The occurrence of destructive earthquakes in the in-land source areas K, F, T, and W is treated as the activities of secondary seismic sources, as discussed in the previous chapter. The intervals between hreat off-shore earthquakes in source P are subdivided into several stages. The earthquakes in the secondary sources are assumed to occur randomly, with occurrence rates assigned to each source and each stage.

Distribution of epicentral locations.—From Fig. 1, it may be observed that there is a close correspondence between the epicentral locations of historical earthquakes and active faults. However, due to the complexity of the tectonic and geological features of the area, it is difficult to identify the causative faults for all earthquakes, particularly for those occuring in the areas covered with thick alluvial deposits. From this, it is assumed in this study that the epicentral locations of earthquakes occurring in the in-land sources K, F, T, and W are statistically independent and uniformly random over each source.

Among the 33 earthquakes registered for source K, the epicentral locations of eight of them have not been identified; it has only been stated that they occurred in the Kyoto area. Considering this, the earthquake occurrence rate for the area within 50 km from the City of Kyoto has been set higher than the other part of source K in proportion to the number of the earthquakes with unknown epicenters relative to the total number.

Magnitude distribution.—The Gutenberg-Richter formula for the relative frequencies of earthquake magnitude is used for the magnitude distribution for the in-land secondary sources; i.e., the number of earthquakes $n/(m)$ whose magnitudes M exceed a value m is given by

$$\log n_M(Mm) = a - bm \quad \cdots\cdots(8)$$

where a and b are constants. Using this, and introducing a lower bound m_0

(significant value in an engineering sense) and an upper bound m_u (limit suggested by the recorded maximum), the distribution function $F_M(m)$ of magnitude is represented[4] by

$$F_M(m) = P(M \leqq m \mid m_0 \leqq M \leqq m_u) = \frac{1-\exp[-2.3b(m-m_0)]}{1-\exp[-2.3b(m_u-m_0)]} \quad \cdots\cdots(9)$$

Table 1 shows the values of the parameters appearing in Eqs. (8) and (9) used in this study, which have been determined from the data in Table A1. The parameter b si said to assume values particular to the specific geological areas. It has been suggested[22] that the b-value averaged for Japan is 1.03, 1.06 for the Pacific side of eastern Japan, 0.72 for the Pacific side of western Japan, and 0.66 generally for the side of the Japan Sea. Compared to these values, the b-values given in Table 1 would be reasonable, except for source W whose sample size is small. For source W, $b=0.6$ is used instead of the value in Table 1.

Table 1. Parameters for Magnitude Distribution for In-land Type Earthquakes

Source area	K	F	T	W
Sample size	33	15	10	4
m	6.0	6.0	6.0	6.0
m_u	8.0	8.0	7.5	7.5
a	7.456	5.777	5.214	2.458
b	0.978	0.766	0.695	0.301
s(*)	0.155	0.051	0.074	0.707

(*) standard error of $\log_{10} n_M(m)$

Nonstationary occurrence rates.—On the basis of the discussion in the previous chapter, the occurrence of in-land earthquakes is modeled in relation to the occurrence of great off-shore earthquakes in the major fault systems. Given a sample value t_r of the interval between two successive great off-shore earthquakes, t_r is subdivided into the following four stages with different earthquake occurrence rates.

(1) Stage I (quiescent period: T_1)
(2) Stage II (low activity period: T_2)
(3) Stage III (active period: T_3)
(4) Stage IV (active period immediately following a huge off-shore earthquake: T_4)

The durations $T_1 \sim T_4$ of these stages are treated as random variables; they follow conditional probability distributions for a given value t_r of the recurrence time T_r of great off-shore earthquakes. Fig. 6 is a schematic illustration of the

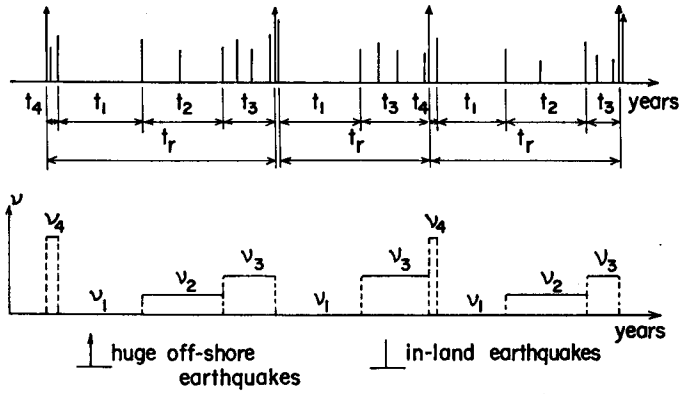

Fig. 6. Illustration of Nonstationary Earthquake Occurrence Model (N-model) for Secondary (In-land) Source Areas.

four stages and a corresponding variation of earthquake occurrence rates. In some cases, Stages II and IV are absent.

The durations of Stages I~IV for each sample value t_r for actual earthquakes have been determined on the basis of the data for source K, for which the most reliable list of historical earthquakes is available. The statistics of the sample values of $t_1 \sim t_4$, their sample means and sample standard deviations are shown along with the values of t_r in Table B1 in Appendix B.

The probability distributions of the random variables T_3 and T_4 have been determined in the following manner. Since these two variables have definite upper and lower bounds, beta distributions have been employed. Their specific forms are given as follows.

(i) The probability density function $f_{T_3}(t_3)$ for the active period T_3 is represented by

$$f_{T_3}(t_3) = \begin{cases} \dfrac{1}{B(1.84,\ 1.48)} \dfrac{(t_3-20)^{0.84}(60-t_3)^{0.48}}{5209}; & 20 \leqq t_3 \leqq 60 \text{ years} \\ 0; \quad \text{elsewhere} \end{cases} \qquad \cdots\cdots\cdots\cdots\cdots\cdots (10)$$

where $B(q, r)$ is the beta function, in which the q- and r-parameters have been determined so that the mean value and the standard deviation of T_3 be equal, respectively, to the sample mean and the sample standard deviation of t_3 in Table B1.

(ii) From Table B1, the active periods immediately following huge off-shore earthquakes are absent with a probability of 0.5; i.e.,

$$P(T_4 = 0) = 0.5 \qquad \cdots\cdots\cdots\cdots\cdots\cdots (11)$$

Otherwise, the conditional probability density $f^*_{T_4}(t_4)$ given that $T_4>0$ is represented by

$$f^*_{T_4}(t_4) = \begin{cases} \dfrac{1}{B(1.0,\ 1.57)} \dfrac{(20-t_4)^{0.57}}{110.3}; & 0<t_4\leqq 20 \text{ years} \\ 0; \quad \text{elsewhere} \end{cases} \qquad \cdots\cdots\cdots(12)$$

in which the q-parameter has been set equal to unity so as to let the mode of T_4 coincide with zero. The r-parameter has been determined so that the mean value T_4 be equal to the sample mean of t_4 in Table B1.

The probability density functions $f_{T_3}(t_3)$ and $f^*_{T_4}(t_4)$ are shown in Fig. 7.

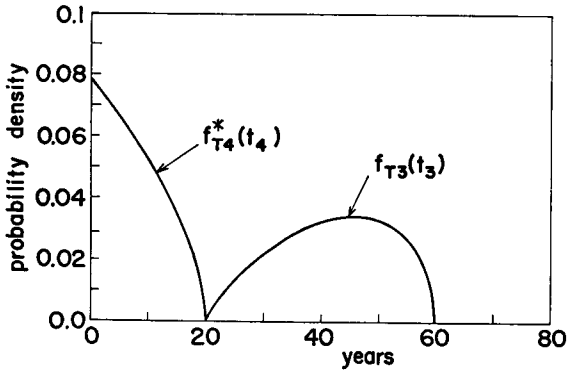

Fig. 7. Probability Density Functions for T_3 and T_4.

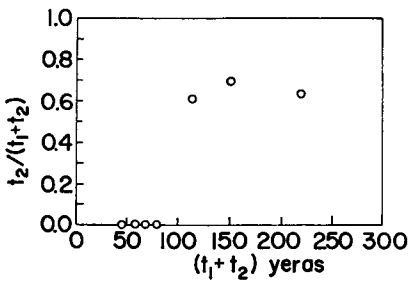

Fig. 8. Relation between Quiescent Period T_1 and Low Activity Period T_2.

The quiescent period T_1 and the low activity period T_2 are determined from T_r, T_3 and T_4. In Fig. 8 which shows the relation between the sample values t_1 and t_2 of the random variables T_1 and T_2, it may be observed that t_2 vanishes when $t_1+t_2<100$ years, whereas t_2 assumes a value around 60~70% of t_2+t_1 if $t_1+t_2<100$ years. Considering that a relation $T_1+T_3=T_r-(T_3+T_4)$ always holds, it is assume that T_1 and T_2 are related deterministically to T_r, T_3 and T_4 in the following manner.

$$\text{(iii)} \quad \left.\begin{array}{l} \text{For } T_r-(T_3+T_4)<100 \text{ years,} \\ \qquad T_2=0 \\ \qquad T_1=T_3-(T_r+T_4) \\ \text{and for } T_r-(T_3+T_4)\geqq 100 \text{ years,} \\ \qquad T_2=0.65[T_r-(t_3+T_4)] \\ \qquad T_1=T_r-(T_2+T_3+T_4) \end{array}\right\} \qquad \cdots\cdots\cdots\cdots(13)$$

The probabilistic models for $T_1 \sim T_4$ have thus been developed. It is assmed that all in-land secondary source areas (K, F, T and W) proceed from one stage to another simultaneously, and that in each stage, the earthquake occurrence in each source area is a Poisson process with an earthquake occurrence rate ν_{ij} for stage i, (i=I, II, III, IV), in source j, (j=K, F, T, W), the probability that n_{ij} destructive earthquakes will occur in source j within a given duration t_i of the stage i is represented by

$$P_{ij}(N_{ij}=n_{ij}) = \frac{(\nu_{ij}t_i)^{n_{ij}}e^{-\nu_{ij}t_i}}{n_{ij}!} \qquad \cdots\cdots\cdots\cdots\cdots\cdots(14)$$

where N_{ij}=random variable for n_{ij}.

It is also assumed that at the time Stage II or Stage III starts, a destructive earthquake will occur in one of the four in-land sources. The probability that the initiating earthquake for the Stage i will occur in source j is given by

$$p_{ij} = \frac{\nu_{ij}}{\sum_j \nu_{ij}} \qquad \cdots\cdots\cdots\cdots\cdots\cdots(15)$$

The occurrence rate ν_{ij} for each stage and each source is given in Table 2.

Table 2. Nonstationary Earthquake Occurrence Rates ν_{ij} for Secondary (In-land) Source Areas (unit: years^{-1})

Stage \ Source area	K	F	T	W
Stage I	0.0	0.0	0.0	0.0
II	0.0223	0.0221	0.0148	0.0148
III	0.0745	0.0734	0.0490	0.0490
IV	0.1284	0.1995	0.2027	0.2994

3. Simulation Model for Seismic Hazard Estimation

3.1 Non-Poisson simulation model

On the basis of the probabilistic model of earthquake occurrence developed in the previous chapter, which is a hierarchical model with combined effects of a major seismic fault system and secondary seismic source areas, a non-Poisson simulation model for a seismic hazard estimation is constituted by combining it with probabilistic attenuation rules.

Monte Carlo simulations for earthquake occurrences are performed in accordandce with the flow chart in Fig. 9. The simulation model is of a memory type in which future earthquake occurrences are simulated on the basis of information on previous seismic activities.

The procedure of simulation is summarized as follows.

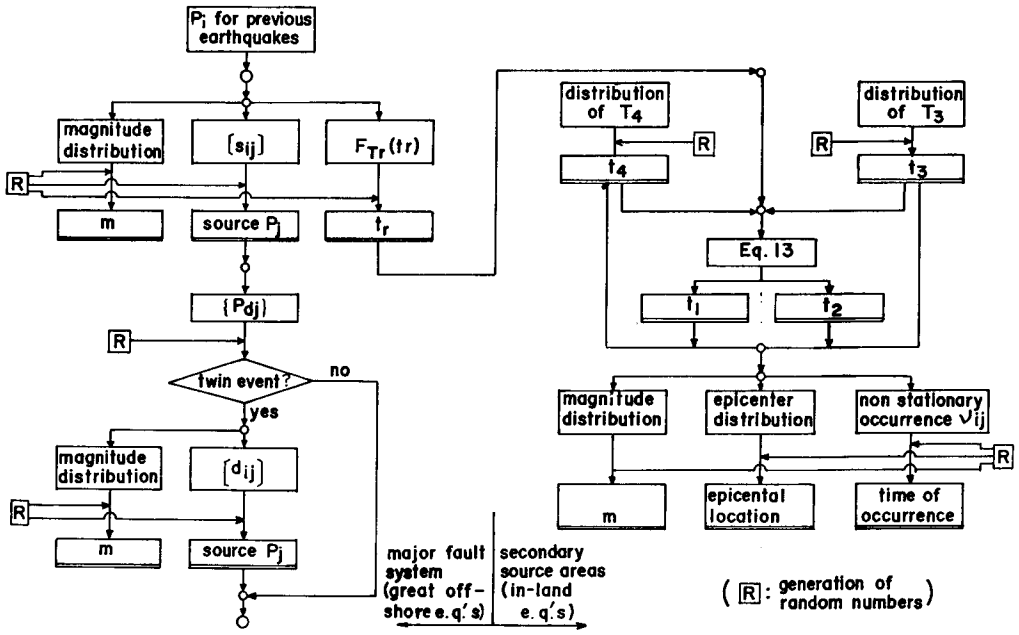

Fig. 9. Illustration of Simulation Model of Non-Poisson Earthquake Occurrences.

Step I: Generation of earthquakes in the major fault system.

(i) A sample value t_r is generated for the recurrence time T_r of great earthquakes in the major off-shore fault system by using the distribution function in Eq. (2).

(ii) On the basis of the source location of the previous earthquake, the nature of the next eqarthquake is determined in a probabilistic manner. The location of the source is determined from Eqs. (6) and (7), and whether or not it is a twin-event is determined from Eq. 5, through generating random numbers.

(iii) The magnitude is determined from the distribution given by Eq. (4).

Step II: Generation of earthquakes in secondary source areas.

The sample value t_r generated in (i) is subdivided into Stages I$\sim$IV in the following manner.

(iv) By using the probability distribution in Eq. (10), a sample value t_3 for the duration T_3 of Stage III is generated. Likewise, a sample value t_4 for the duration T_4 of Stage IV is generated by using Eqs. (11) and (12).

(v) Sample values t_1 and t_2 of the durations T_1 and T_2, respectivdley, of Stages I and II are determined from Eq. (13) by replacing $T_1\sim T_4$ and T_r by $t_1\sim t_4$ and t_r, respectively.

(vi) At the time when Stage II (only when $T_2>0$) or Stage III starts, an earthquake is generated in one of the source areas determined randomly, by using the probability distribution in Eq. (15).

(vii) Sample numbers n_{ij} of earthquakes occurring in the source areas K, F, T and W for Stages II~III are generated by using the probability distribution in Eq. (14).

(viii) The epicentral locations and the times of occurrence of the n_{ij} earthquakes are determined through a uniform random distribution over source j and Stage i.

(ix) Their magnitudes are generated by using the probability distribution in Eq. (9).

Fig. 10 shows an example of a smaple time series of simulated earthquake occurrences, which have been generated for 1000 years under a condition that a great off-shore earthquake occurred at $t=0$ in source P_1. It may be observed that the overall characteristics of the earthquake history in Fig. 2 have been reproduced satisfactorily in Fig. 10.

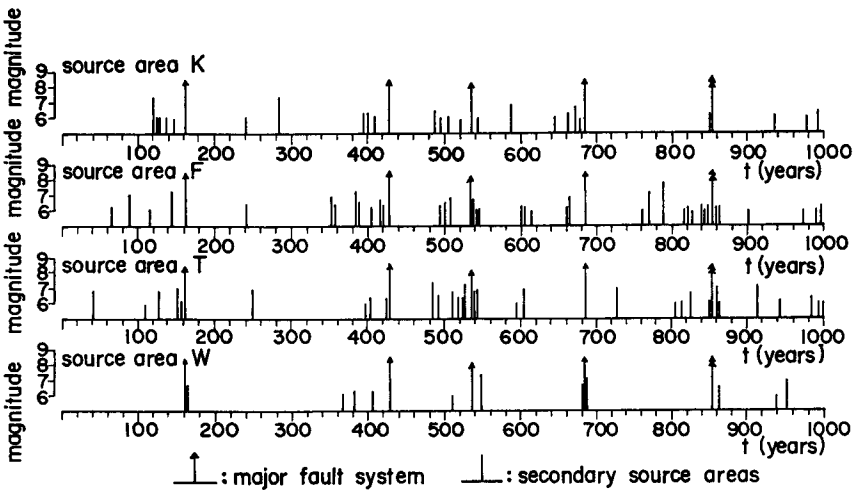

Fig. 10. Sample Time Series of Simulated Earthquakes.

3.2 Equivalent Poisson model

In the subsequent part of this study, the non-Poisson model developed above will be discussed often in comparison with conventional Poisson-type models. For this purpose, the equivalent Poisson model is identified as follows.

Distribution of epicentral locations.—The epicenters of the earthquakes in the secondary in-land sources are distributed randomly, exactly in the same manner

as in the non-Poisson model. The source migration of great off-shore earthquakes in source P is assumed to be independent and uniformly random.

Magnitude distribution.—The probability distribution of earthquake magnitudes for each source is identical with that in the non-Poisson model.

Occurrence rates.—The stationary Poisson occurrence rate ν_{0j} for source j, (j=K, F, T, W), determined from the data in Table A1 is shown in Table 3.

Table 3. Earthquake Occurrence Rates for Equivalent Poisson-Type Model (unit: years^{-1})

Source area	K	F	T	W	P
Occurrence rate	0.0302	0.0401	0.0267	0.0107	0.0094

3.3 Attenuation model

Attenuation models to estimate the ground motion Y for a given magnitude m and a given source-to-sive distance r are generally represented in the form

$$Y = Uy_c(m, r) \qquad \cdots\cdots(16)$$

where $y_c(m, r)$=attenuation equation which is the conditional mean value of Y for given and m r, and U=random variable to account for the attenuation uncertainties.

A number of works[5,8,13,16,21] have been performed to develop attenuation models of the form of Eq. (16), using various regression equations and various datasets of strong motion records. What form of attenuation models should be used will depend on the purpose of each study.

Herein, the attenuation model developed by Goto, Kameda, Imanishi and Hashimoto[8] is used. It is based on the strong motion data recorded in Japan, and instrument- and baseline-corrected. Then the peak ground acceleration A and the peak ground velocity V, both being random variables, for a given magnitude m and a given epicentral distance Δ (in km) are represented by*

$$A = U_a a_c(m, \Delta) \qquad \cdots\cdots(17)$$

where

$$a_c(m, \Delta) = 407 \times 10^{0.16m}/(\Delta+30)^{0.752}, \quad \text{(gal)} \qquad \cdots\cdots(18)$$

and

$$V = U_v v_c(m, \Delta) \qquad \cdots\cdots(19)$$

where

$$v_c(m, \Delta) = 4.97 \times 10^{0.20m}/(\Delta+30)^{0.530}, \quad \text{(kine)} \qquad \cdots\cdots(20)$$

* 1 gal=1 cm/sec^2, and 1 kine=1 cm/sec.

The random variables U_a and U_v are treated as lognormal variates; i.e., ln U_a and ln U_v are normal variates, and their mean value and standard deviation are given as

$$\mu(\ln U_a) = 0\,, \quad \sigma(\ln U_a) = 0.443 \qquad \cdots\cdots(21)$$

$$\mu(\ln U_v) = 0\,, \quad \sigma(\ln U_v) = 0.746 \qquad \cdots\cdots(22)$$

For each simulated sample earthquake occurrence, sample ground motions (acceleration and velocity) for arbitrary sites are generated by using the attenuation model characterized by Eqs. (17)~(22).

3.4 Verification of the non-Poisson model

Besides the direct comparison of the recorded and simulated time series of earthquakes using Figs. 2 and 10, the non-Poisson earthquake occurrence model developed herein is tested from the recurrence time distribution of earthquakes observed at a fixed site.

Fig. 11, prepared by Kameda and Ozaki[12] shows the recurrence time distribution of the earthquakes felt to be of intensities no less than V in the JMA (Japan Meteorological Agency) scale in Kyoto City. (JMA and MM scales are

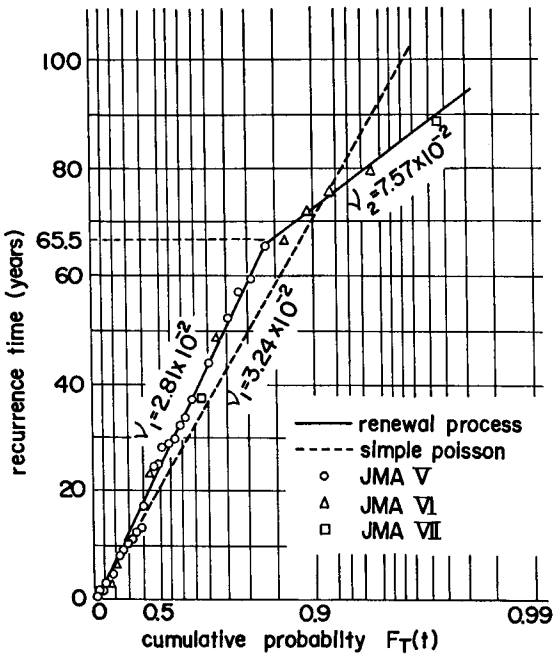

Fig. 11. Recurrence Time Distribution of Earthquakes in Kyoto (JMA intensity $\geq$ V; Ref. 12).

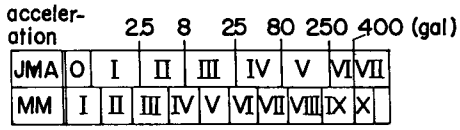

Fig. 12. JMA and MM Intensity Scales.

compared in Fig. 12.) On the basis of this figure, it has been pointed out[12] that the destructive earthquakes which attacked Kyoto have not occurred in a Poisson process, but in a certain renewal process that can be modeled with two stages of Poisson processes. That is, for 65.5 years following an earthquake, subsequent earthquakes will occur in a Poisson process with an occurrence rate ν_1, but if no earthquakes occur during this 65.5 year period, the occurrence rate for the next earthquake will be ν_2 (larger than ν_1). This feature is expressed by the two solid lines in Fig. 11. If the earthquakes had occurred in a Poisson process, the data points should have lain on a straight line.

Simulations of ground accelerations for Kyoto City for a time span of 1000 years have been repeated, using the non-Poisson model and the equivalent Poisson model developed above. Then, the accelerations have been converted to the JMA intensity based on Fig. 12. For each simulation of 1000 years, a recurrence time distribution has been obtained for simulated earthquakes with JMA intensities no less than V in Kyoto City. An example is shown in Fig. 13. Note that a

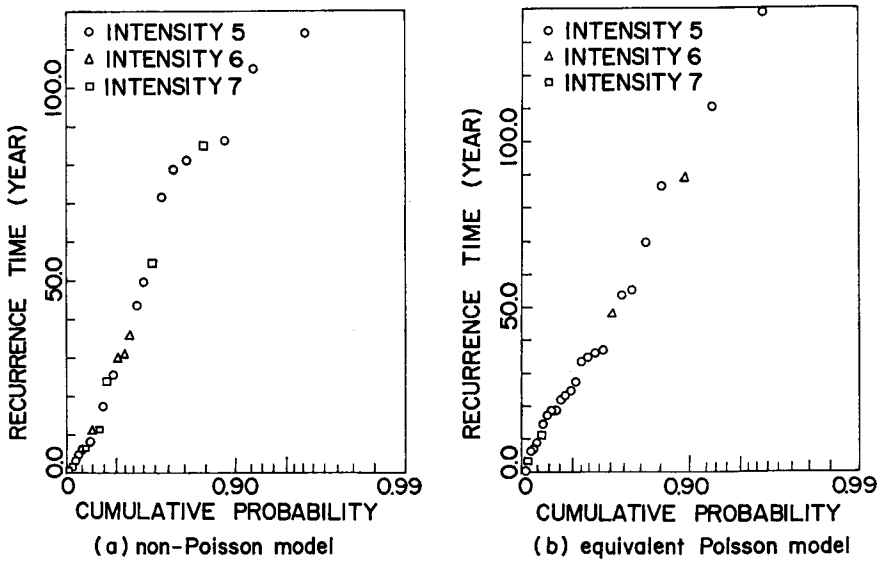

Fig. 13. Recurrence Time Distribution of Simulated Earthquakes with JMA intensity $\geqq$ V in Kyoto.

clear break point is observed in the simulated data in Fig. 13(a), based on the non-Poisson model, whereas the data in Fig. 13(b), based on the equivalent Poisson model, lie generally on a single straight line. The similarity between Fig. 11 and Fig. 13(a) should demonstrate the appropriateness of the non-Poisson model developed in this study.

Of the ten sample distributions obtained for the non-Poisson model, the break point such as that observed in Fig. 13(a) did not always appear. Therefore, the recurrence time distribution suggested by actual earthquakes in Fig. 11 may not be a stable one for a very long time span. Nevertheless, the above arguments will be a reason to verify the non-Poisson model if we consider that none of the results for the equivalent Poisson model showed such break points; their data always lay on single straight lines.

4. Results of Simulation for the Kinki District

4.1 Outline of simulation analysis

The non-Poisson simulation model has been applied to the seismic hazard estimation for the Kinki District with has been focused on throughout this study. As has been emphasized repeatedly, it is expected that useful information will be provided regarding the future seismic risk along the time axis with the origin at any absolute time, something that can not be obtained from conventional Poisson-type models.

As to the origin of time t of a future period, the following five cases have been considered.

Case 1: $t=0$ at the start of Stage I (quiescent period).
Case 2: $t=0$ at the start of Stage II (low activity period).
Case 3: $t=0$ at the start of Stage III (active period)
Case 4: $t=0$ at the start of Stage IV (active period immediately following a great off-shore earthquake).
Case 5: $t=0$ in January 1979.

With the aid of the analysis for Cases 1$\sim$4, the significance of the non-Poisson model will be demonstrated, as these cases sketch the overall variations of the future seismic risk throughout a cycle of the seismic activities of the area. The time origin in Case 5, January 1979, is regarded to be 32.0 years after a great off-shore earthquake which occurred in 1946 in source P_1, 26.5 years after entering Stage I, and is still in Stage I.

Simulations have been performed for the future periods of $t=5$, 10, 20, 30, 40, 50, 75, 100, 150, and 200 years. The number of simulations n_s has been chosen as

$n_s = 2000$ for $t \leqq 50$ years, and

$n_s = 1000$ for $t > 50$ years,

after examining the convergence of parameters to be generated, as the resulting information.

In the following sections, the results of the simulations will be presented and discussed from various points of view, particularly on the effect of the periodicity and the nonstationarity of the seismic activities considered in the non-Poisson model, and on the probabilistic models of seismic hazards for the Kyoto-Osaka area.

4.2 Expected number of earthquakes

Fig. 14 shows the mean number of destructive earthquakes for the whole Kinki District. Whereas all values for Cases 1～5 have been obtained from Monte Carlo simulations, the result for the equivalent Poisson model has been calculated from a simple expression $\nu_0 t$, in which ν_0 denotes the sum of all values of ν_{0j} in Table 3.

The results for Cases 1～5 in Fig. 14 demonstrate the effect of introducing an absolute time axis through the use of the non-Poisson model. In Case 1, where $t=0$ corresponds to the start of Stage I (quiescent period), the mean number of

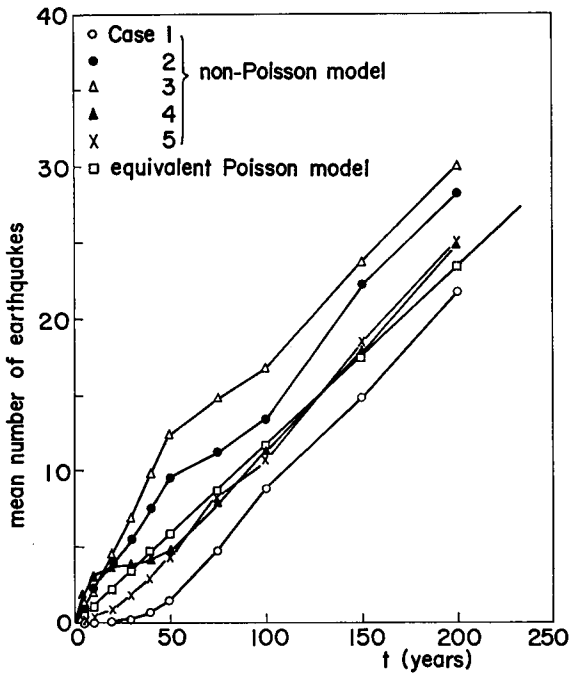

Fig. 14. Mean Number of Earthquakes for the Kinki District.

earthquakes for the first 50 years remains quite small, after which it begins to increase as Stages II and III emerge, yet remaining generally below the result for the equivalent Poisson model. In Cases 2 and 3, where $t=0$ corresponds, respectively, to the start of Stage II (low activity period) and Stage III (active period), the mean number of earthquakes assumes values larger than that for the equivalent Poisson model. The difference between these two extreme cases are particularly large with in a time range of some 75 years. Cases 4 and 5 are for some intermediate situations between these extreme cases, and as a result they happen to agree fairly well with the results for the equivalent Poisson model. These effects of the initial conditions in a simulation using the non-Poisson model will be discussed again in the next section, in relation to the mean maximum ground motions.

Among the mean total number of earthquakes to occur in the whole Kinki District, a limited number of them will have appreciable effects on a specific site. Fig. 15 shows the mean number of earthquakes that will cause ground motions in Kyoto City exceeding various levels of acceleration.

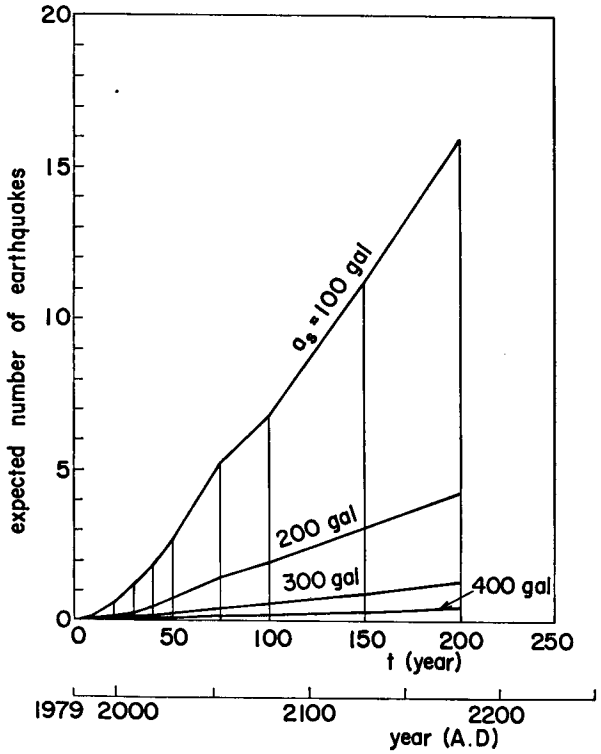

Fig. 15. Expected Number of Earthquakes with Accelerations Exceeding a_s (Case 5; Kyoto).

4.3 Mean maximum ground motions

Fig. 16 shows the mean values and the standard deviations of the maximum ground acceleration and the maximum ground velocity to occur in Kyoto City in the future t years. Observe again that the mean maximum ground motions within the range $t<100$ years are greatly affected by the initial conditions at $t=0$. At $t=50$ years, for example, acceleration for Case 3 is approximately three times that for Case 1. The ratio for the mean maximum velocity is even as large as four. The equivalent Poisson model naturally gives results somewhat averaging the various cases of the non-Poisson model.

The mean maximum ground motion for all cases tend to approach the results for the equivalent Poisson model as t increases. This can be regarded as a consequence of "time averaging", effected by finishing a complete cycle of the seismic activities consisting of the four Stages in the secondary in-land sources, and an occurrence of a great off-shore earthquake in the major fault system P.

At least $t=100$ years for the acceleration, and $t=200$ years for the velocity will be needed for this time averaging process to be finished. The results for the equivalent Poisson model can represent those for all cases with a non-Poisson model. These time spans are so long that they are in the range of required useful lives of special engineering structures of primary importance. Many other structures and facilities are only required to have shorter lifetimes. For them, the expected seismic loads suggested by the non-Poisson model will be considerably different from what is estimated from simple Poisson process models. In such cases, it will be significant to make engineering judgments on the seismic risk, based on the results from the non-Poisson models such as that developed herein. Despite the somewhat greater complexity of the model, use of the non-Poisson model will be rewarded by useful information pertaining to the seismic risk for particular times and periods.

Fig. 16 also shows the standard deviations of the maximum ground motions in Kyoto. It is observed that, except for Case 1, the standard deviations for all other cases agree well and that they assume fairly constant values for t. In Case 1, the standard deviations increase with t in the range $t<50$ years, whereas for $t>50$ years they behave in the same manner as in the other cases.

Figs. 17 and 18 show resutls similar to Fig. 16, but for Case 5, values observed from January 1979, for Kyoto and Osaka, respectively. It may be noted that January 1979 is still in Stage I, but its future seismic risk has increased from that in Case 1 to a level closer to the results of the equivalent Poisson model.

Fig. 19 shows the geographical distribution of the mean maximum acceleration

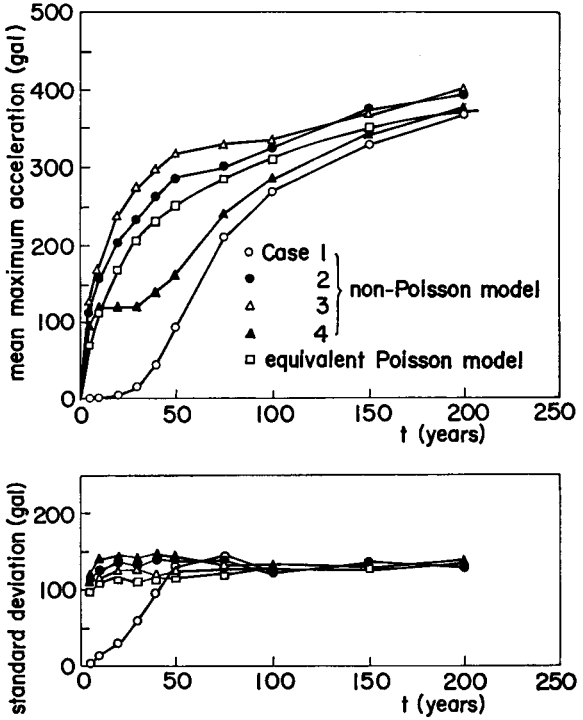

Fig. 16(a). Mean Value and Standard Deviation of Maximum Acceleration (Case 1–4; Kyoto).

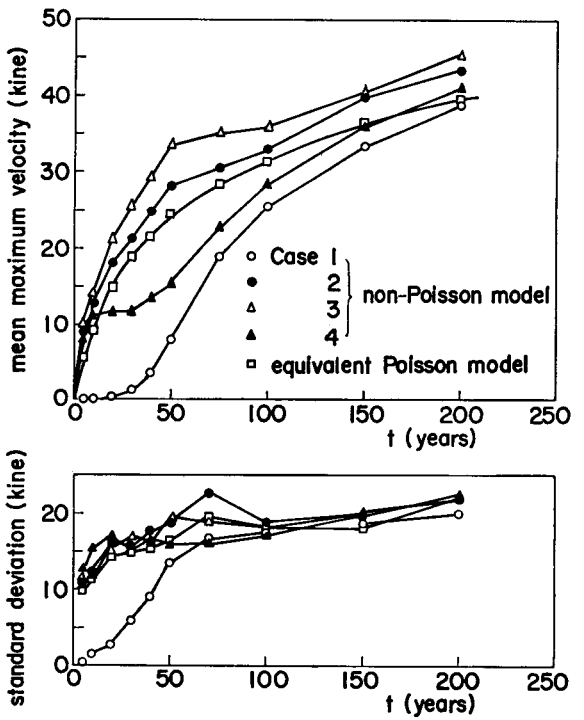

Fig. 16(b). Mean Value and Standard Deviation of Maximum Velocity (Cases 1–4; Kyoto).

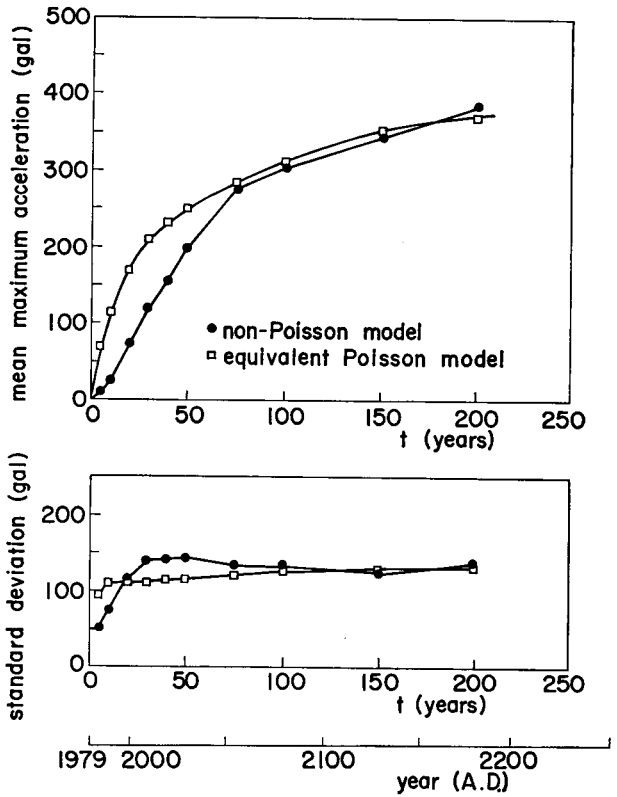

Fig. 17(a). Mean Value and Standard Deviation of Maximum Acceleration (Case 5; Kyoto).

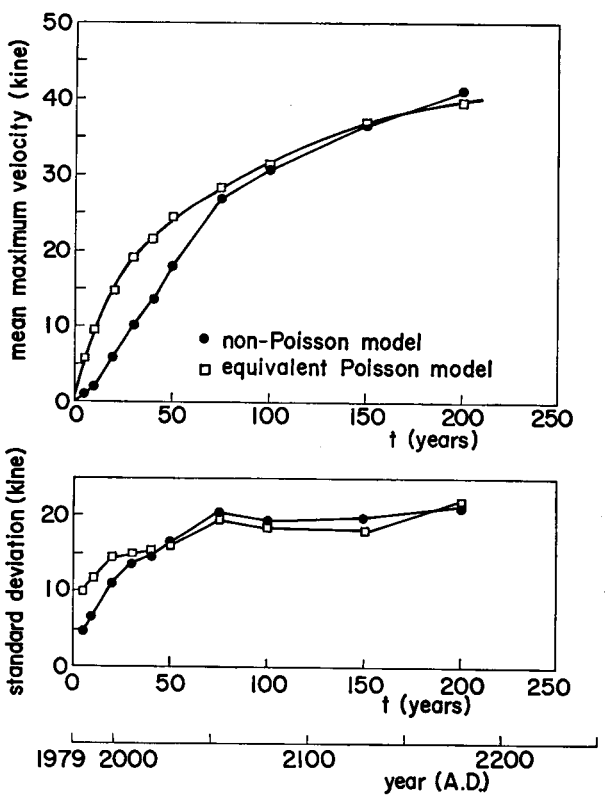

Fig. 17(b). Mean Value and Standard Deviation of Maximum Velocity (Case 5; Kyoto).

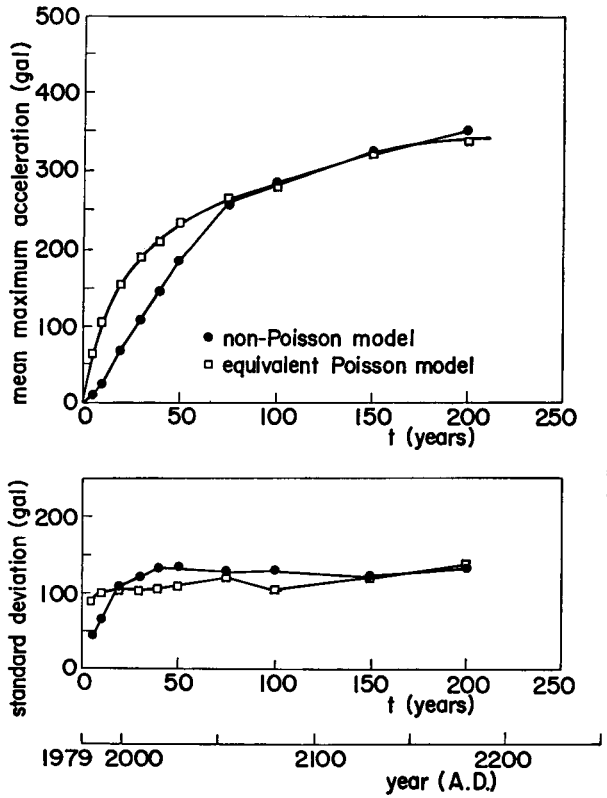

Fig. 18(a). Mean Value and Standard Deviation of Maximum Acceleration (Case 5; Osaka).

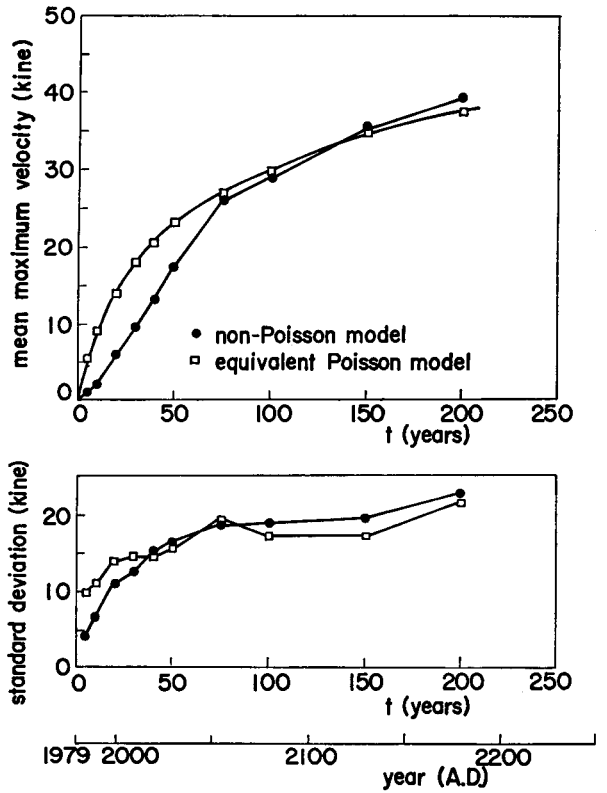

Fig. 18(b). Mean Value and Standard Deviation of Maximum Velocity (Case 5; Osaka).

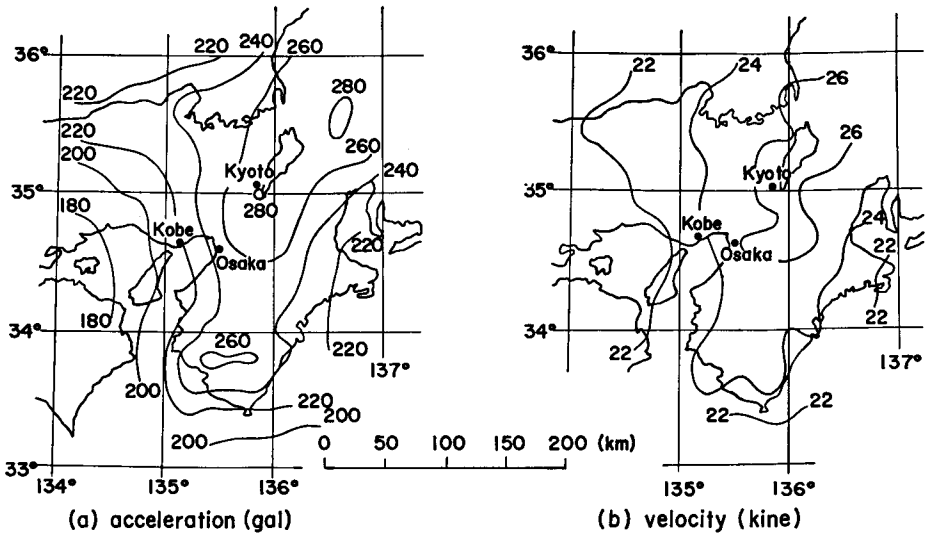

Fig. 19. Mean Maximum Ground Motions of the Kinki District (Case 5; observed from Jan. 1979, t=75 years).

and the mean maximum velocity for a future period t=75 years, observed from January 1979, Case 5. The distribution of velocity is much more uniform than that of acceleration. This is a consequence of the attenuation model characterized by Eqs. (17)~(22), in whicn the attenuation of velocity with the epicentral distance is slower than that of acceleration, and the attenuation uncertainty for the velocity represented by $\sigma(\ln U_v)$ is larger than that for acceleration, $\sigma(\ln U_a)$.

4.4 Contribution of specific sources to site ground motions

In repeating the simulation procedure for n_s times, the maximum ground motion within t years generated from each simulation is caused by an earthquake occurring in any of the sources K, F, T, W, and P. The relative frequency of earthquakes occurring in a specific source causing the maximum ground motion at a certain site will represent the contribution from that source to the site. The contribution factor r_{nj} from source j is defined by

$$r_{nj} = n_{sj}/(n_s - n_{s0}) \qquad \cdots\cdots(23)$$

where n_s=number of simulations, n_{s0}=number of simulations in which no sample earthquakes have been generated, and n_{sj}=number of simulations in which the maximum ground motion at the site was caused by an earthquake in source j. It is clear that r_{nj} satisfies

$$\sum_j r_{nj} = 1 \qquad \cdots\cdots(24)$$

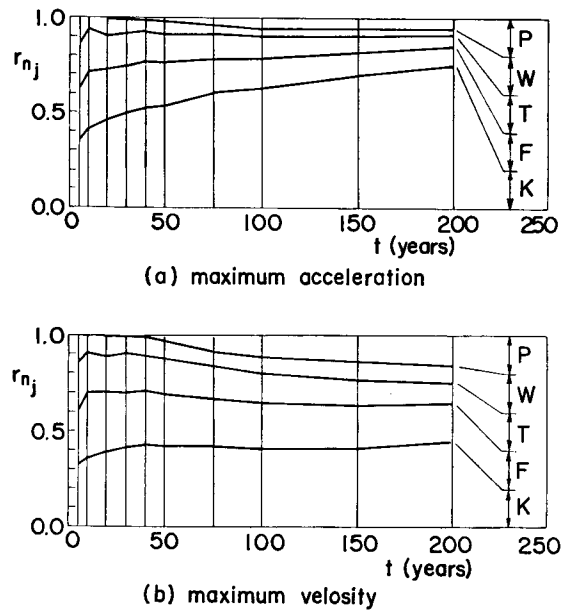

Fig. 20. Contribution of Source Areas to Maximum Ground Motion in Kyoto (Case 5).

Fig. 20 shows the contribution factor r_{nj} for the ground motions in Kyoto for Case 5, demonstrating that the contribution factor varies with time. In Fig. 20(a), which shows the effect on the maximum acceleration, the contribution from source K that contains Kyoto is pronounced. The value of r_{nj} for source K increases with t as active periods are experienced. This result would imply that the maximum acceleration will be affected rather by close earthquakes of moderate magnitude than great distant earthquakes. From Fig. 20(b), on the other hand, it may be observed that there are considerable contributions from other sources to the maximum velocity. This is again the effect of a slow attenuation of ground velocity with the distance. Note particularly that the contribution from source P increases for values of t larger than 50 years as the probability of occurrences of great offshore eqarthquakes increases.

4.5 Probabilistic model of maximum ground motions

Fig. 21 shows plots of the simulated maximum accelerations in Kyoto on a lognormal probability paper and a Gumbel probability paper. Both of these distributions are generally acceptable. However, from comparing many similar cases for other sites, it has been concluded that the lognormal distribution is more suitable for the probability distribution of the maximum ground motions dealt with in the simulation model developed herein.

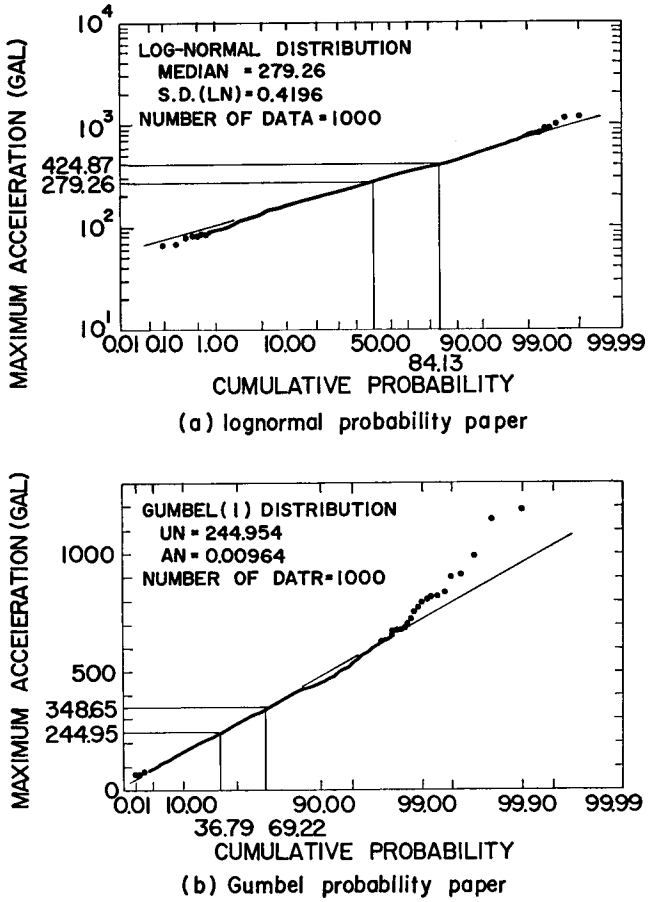

Fig. 21. Probability Distribution of Maximum Acceleration in Kyoto (Case 5; observed from Jan. 1979, $t=100$ years).

It is noted that the distributions shown in Fig. 21 are conditional distributions, given that at least one destructive earthquakes have occurred in any of the sources. Therefore, if this conditional distribution is denoted by $F_{Y_m}(y_m; t \mid \mathrm{E}_1) = P(Y_m \leqq y_m; t \mid \mathrm{E}_1)$, in which E_1 denotes an occurrence of an earthquake, then the distribution function of the maximum ground motion Y_m in the future t years is represented by

$$F_{Y_m}(y_m; t) = p_0 + (1-p_0) F_{Y_m}(y_m; t \mid \mathrm{E}_1) \quad \cdots\cdots(25)$$

where

$$p_0 = P(\bar{E}_1) = P \text{ (no earthquakes)} \quad \cdots\cdots(26)$$

The probability p_0 is obtained from

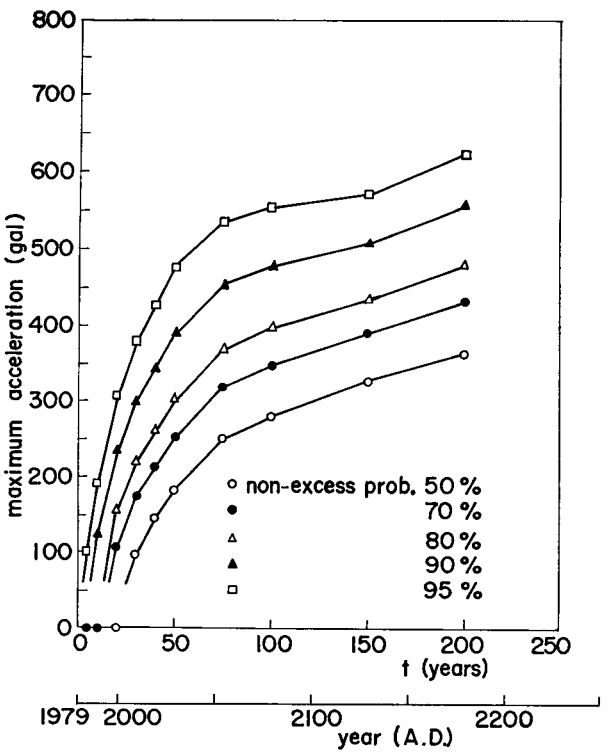

Fig. 22(a). Probability-Consistent Maximum Acceleration (Case 5; Kyoto).

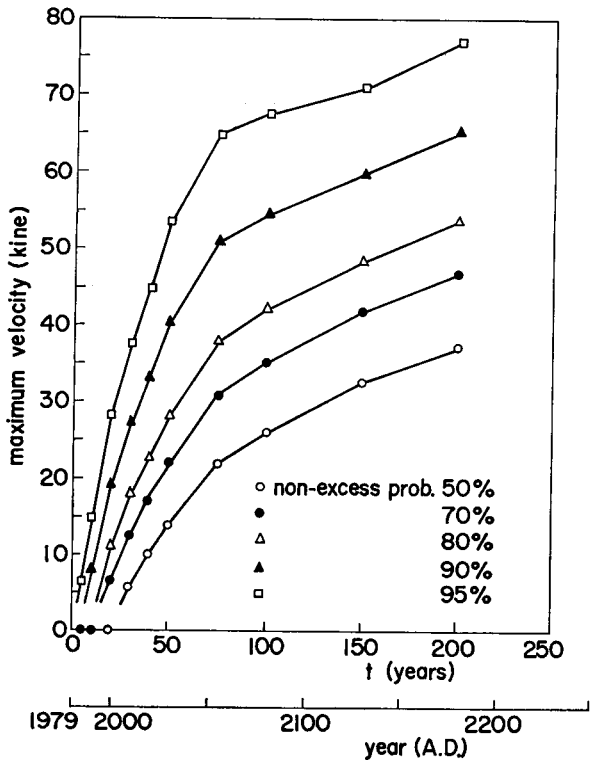

Fig. 22(b). Probability-Consistent Maximum Velocity (Case 5; Kyoto).

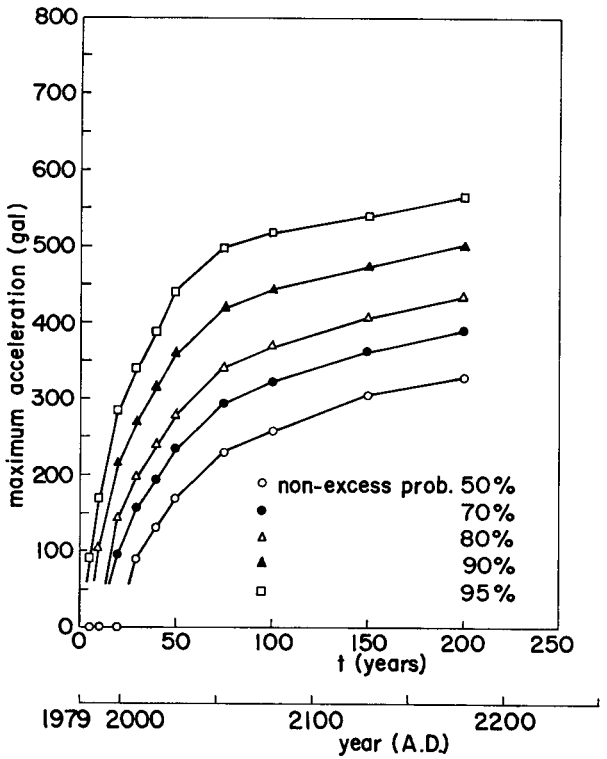

Fig. 23(a). Probability-Consistent Maximum Acceleration (Case 5; Osaka).

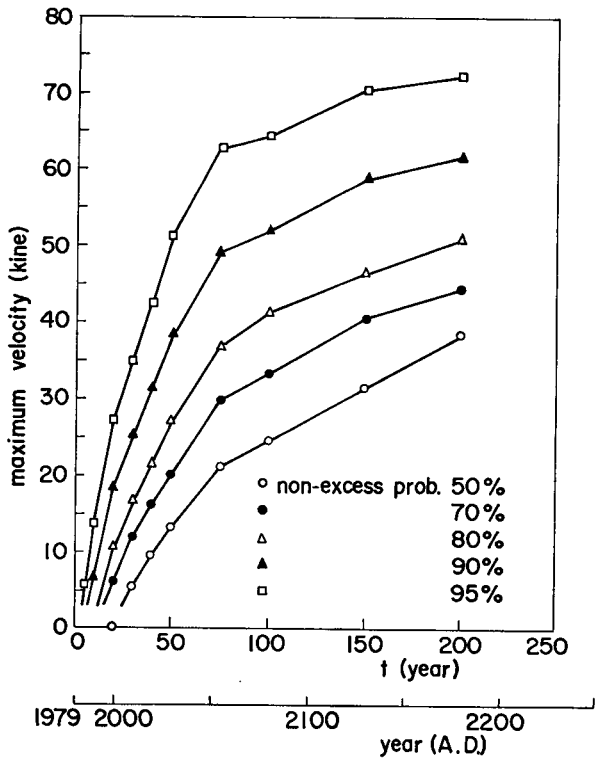

Fig. 23(b). Probability-Consistent Maximum Velocity (Case 5; Osaka).

$$p_0 = \frac{n_{s0}}{n_s} = 1 - \frac{n_{s1}}{n_s} \qquad \cdots\cdots\cdots\cdots\cdots\cdots (27)$$

in which $n_{s1}=n_s-n_{s0}$.

In Table C1 in Appendix C, the results of simulations and the reduced parameters needed for establishing probabilistic models are listed for the maximum acceleration and the maximum velocity in Kyoto and Osaka, and for various values of future yt years observed from January 1979.

By using the lognormal distribution modeled in Table C1 and Eq. (25), the values of acceleration and velocity corresponding to various non-excess probabilities are shown in Figs. 22 and 23 for Kyoto and Osaka, respectively, for the future period t starting from 1979.

5. Conclusions

Major results of this study may be summarized as follows.

(1) A non-Poisson simulation model for a seismic hazard estimation has been developed, that accounts for the periodicity and the nonstationarity of seismic activities. The model is a combination of a renewal process model (R-model) for great earthquakes occurring in major fault systems, and nonstationary Poisson occurrences (N-model) of other destructive earthquakes in secondary source areas.

(2) The non-Poisson model has been developed on the basis of the earthquake history in the Kinki District, a western part of Japan that contains the Kyoto-Osaka-Kobe metropolitan area. The developed model has been applied extensively to the area.

(3) Through the application of the non-Poisson model, various kinds of information useful for engineering seismic risk evaluation have been obtained. Particularly, information on the future seismic risk based on the present stage of seismic activities would be of interest, that can not be obtained from conventional Poisson-type models. Through discussions of these results, the significance of the non-Poisson model has been demonstrated.

(4) In estimating seismic hazards, site acceleration and site velocity have been dealt with by using different probabilistic attenuation rules. The results of simulation demonstrate the effect of slow attenuation of the velocity with distance compared to the acceleration. That is to say far field earthquakes contribute significantly to the site velocities, whereas site accelerations are determined primarily by closer earthquakes.

It has been emphasized throughout this study that the Poisson-type models are often an oversimplification of actual phenomena in assessing the seismic risk for

a future period for engineering purposes. For this reason, the non-Poisson model has been developed in this study. It should be pointed out, however, that considerable simplifications have also been made in establishing the non-Poisson model. For example, a stepwise variation of the occurrence rates has been assumed in the N-model, whereas in actual cases the variation should be continuous. The hierarchical relation between the major fault system and the secondary source employed in this study may be of a more interactive nature in the real world. Moreover, there can be an influence of major faults in other plate boundaries that have been neglected in this study, for example those in the eastern part of Japan. Depsite these simplifications, the non-Poisson model developed in this study should be significant for an engineering analysis as a first order approximation of the periodicity and the nonstationarity of seismic activities.

It may be pointed out that the simulation model developed herein is primarily for macrozoning of seismic risk. The model will be of practical value when it is used in combination with a technique of microzoning. Many works have been conducted on microzonation (Ref. 19). A work has been done by a group including the senior author (Ref. 9) to perform microzonation making use of the soil data for specific sites in an effective way. Works combining macrozoning and microzoning using these methods will be presented elsewhere.

Finally, it is noted that the peak instrumental accelerations are not necessarily a direct measure of destructiveness of earthquake motions. A concept of equivalent peak acceleration (EPA) has been proposed and incorporated in design provisions (Ref. 2). However, an appropriate definition of the EPA has not yet been established. Work is underway to identify paramaters to represent the hazard potential of ground motions in simple acceleration terms. With those parameters, it is planned to perform seismic hazard estimations using the non-Poisson model developed herein.

References

1) Ang, A. H-S., and Tang, W.H., "Probability Concepts in Engineering Planning and Design," John Wiley, 1975.
2) Applied Technology Council, "Tentative Provisions for the Development of Seismic Regulations for Buildings," June 1978.
3) Cornell, C.A., "Engineering Seismic Risk Analysis," *Bulletin of the Seismological Society of America*, Vol. 58, No. 5, Oct. 1968, pp. 1583–1606.
4) Der-Kiureghian, A., and Ang, A. H-S., "A Fault-Rupture Model for Seismic Risk Analysis," *Bulletin of the Seismological Society of America*, Vol. 67, No. 4, Aug. 1977, pp. 1173–1194.
5) Donovan, N.C., "A Statistical Evaluation of Strong Motion Data Including the February 9, 1971 San Fernando Earthquake," *Proceedings*, 5th World Conference on Earthquake Engineering, Rome, 1973, Vol. 1, 1974, pp. 1252–1261.

6) Donovan, N.C., Bolt, B.A., and Whitman, R.V., "Development of Expectancy Maps and Risk Analysis," *Journal of the Structural Division*, ASCE, Vol. 104, No. ST8, Aug. 1978, pp. 1179–1192.
7) Goto, H., and Kameda, H., "Statistical Inference of Future Earthquake Ground Motions," *Proceedings*, 4th World Conference on Earthquake Engineering, Santiago, 1969, Vol. 1.
8) Goto, H., Kameda, H., Imanishi, N., and Hashimoto, O., "Statistical Analysis of Earthquake Ground Motion With the Effect of Frequency Content Correction," *Proceedings*, 5th Japan Earthquake Engineering Symposium, Tokyo, Nov. 1978, pp. 49–56.
9) Goto, H., Sugito, M., Kameda, H., and Isoda, A., "Microzoning for Seismic Risk Analysis of Lifeline Systems," to appear in the *Annuals*, Disaster Prevention Research Institute, Kyoto University, No. 24B, Apr. 1981.
10) Hattori, S., "Regional Distribution of Presumable Maximum Earthquake Motions at the Base Rock in the Whole Vicinity of Japan," *Bulletin of the International Institute of Seismology and Earthquake Engineering*, Vol. 14, 1976, pp. 47–86.
11) Ishibashi, K., "Time Dependence of Seismic Activities in the Tokyo Metroplitan area," *the News of the Japan Society for Earthquake Engineering Promotion*, No. 45, Feb. 1979, pp. 26–28, (in Japanese).
12) Kameda, H., and Ozaki, Y., "A Renewal Process Model for Use in Seismic Risk Analysis," *Memoirs of the Faculty of Engineering*, Kyoto University, Vol. 41, Part 1, Jan. 1979, pp. 11–35.
13) Katayama, T., "Statistical Analysis of Peak Accelerations of Recorded Earthquake Motions," *Seisan Kenkyu*, Institute of Industrial Science, University of Tokyo, Vol. 26, No. 1, Jan. 1974, pp. 18–20.
14) Katayama, T., "Distribution of Structure's-Period-Dependent Seismic Risk in Japan," *Proceedings*, 7th World Conference on Earthquake Engineering, Istanbul, Vol. 1, Sep. 1980, pp. 331–330.
15) Kawasumi, H., "Measures of Earthquake Danger and Expectancy of Maximum Intensity Throughout Japan as Inferred from the Seismic Activity," *Bulletin of the Earthquake Research Institute*, Vol. 29, 1951, pp. 469–482.
16) McGurire, R.K., "Seismic Structural Response Risk Analysis, Incorporating Response Regressions on Earthquake Magnitude and Distance," Structures Publication, No. 399, Department of Civil Engineering, Massachussetts Institute of Technology, Aug. 1974.
17) Nishioka, T., and Shah, H.C., "Application of the Markov Chain on Probability of Earthquake Occurrence," *Proceedings*, JSCE, No. 298, June 1980, pp. 137–145.
18) Ozawa, I., "Estimated Seismic Activities in Kyoto City and Its Vicinity," June 1977, (in Japanese).
19) Proceedings of the 2nd International Conference on Microzonation, San Francisco, 1978.
20) Scawthorn, C., Yamada, Y., and Iemura, H., "Seismic Risk Analysis of Urban Regions," *Proceedings*, 5th Japan Earthquake Engineering Symposium, Nov. 1978, pp. 57–64.
21) Trifunac, M.D., and Brady, A.G., "On the Correlation of Peak Acceleration of Strong Motion with Earthquake Magnitude, Epicentral Distance and Site Conditions," *Proceedings*, U.S. National Conference on Earthquake Engineering, 1975, pp. 43–52.
22) Tsuboi, T., "Earthquakes," Iwanami, 1967, (in Japanese).
23) Usami, T., "Catalogue of Japanese Disastrous Earthquakes," University of Tokyo Press, 1975, (in Japanese).

Appendix A. Table A1. Historical Earthquakes for the Kinki District

Series No.	Date		Epicentral location		Magnitide	Source area	Epicentral distance to Kyoto (km)	JMA intensity in Kyoto
	Year (A.D.)	Month, day	Longitude (°E)	Latitude (°N)				
1	887	8.26	135.3	33.0	8.6	P	220	5
2	890	7.10	Kyoto		6.2	K	0	5
3	934	7.16	Kyoto		6.2	K	0	5
4	938	5.22	135.8	34.8	6.9	K	5～10	6
5	976	7.22	135.8	34.9	6.7	K	5	7
6	1038	1.30	135.6	34.3	6.7	K		
7	1041	8.25	Kyoto		6.4	K		5
8	1070	12.1	135.8	34.8	6.4	K	5～10	4～5
9	1091	9.28	135.8	34.3	6.2	K	65	5
10	1093	3.19	Kyoto		6.4	K		5
11	1096	12.17	137.2	34.2	8.4	P	220	5
12	1099	2.27	135.5	33.0	8.0	P	220	4
13	1177	11.26	135.8	34.7	6.2	K	10	4
14	1185	8.12	136.1	35.3	7.4	K	35	7
15	1245	8.27	Kyoto		6.2	K		5
16	1317	2.24	135.8	35.1	6.7	K		6～7
17	1325	12.5	136.1	35.6	6.7	K		
18	1331	8.15	135.2	33.7	7.0	W		
19	1350	7.6	Kyoto		6.2	K		5
20	1361	8.3	135.0	33.0	8.4	P	205	5
21	1369	9.7	Kyoto		6.1	K		5
22	1449	5.13	135.75	35.0	6.4	K		6
23	1494	6.19	135.7	34.6	6.4	K	30	4～5
24	1498	9.20	138.2	34.1	8.6	P	240	5
25	1510	9.21	135.7	34.6	6.7	K	30	5
26	1579	2.25	135.7	34.7	6.2	K		
27	1596	9.5	135.75	34.85	7.0	K		7
28	1605	2.3	134.9	33.0	7.9	P	260	4
29	1639	—	136.2	35.9	6.1	F		
30	1640	11.23	136.2	36.2	6.7	F		
31	1662	6.16	136.0	35.25	7.6	K	30	6
32	1664	8.3	Kii•Kumano		6.6	W		
33	1665	6.26	Kyoto		6.1	K		5
34	1691	—	136.3	36.3	6.2	F		
35	1694	12.12	Tango		6.1	T		5
36	1707	10.28	135.9	33.2	8.4	P	170	5
37	1710	10.3	133.8	35.5	6.6	T		
38	1711	3.19	133.8	35.4	6.6	T		
39	1715	2.1	136.6	35.4	6.2	F		
40	1715	3.26	135.4	35.0	6.4	K	20	5
41	1819	8.2	136.3	35.2	7.4	K	48	4

Table A1. (countinued)

Series No.	Date		Epicentral location		Magnitide	Source area	Epicentral Distance to Kyoto (km)	JMA intensity in Kyoto
	Year (A.D.)	Month, day	Longitude (°E)	Latitude (°N)				
42	1830	8.19	135.7	35.0	6.4	K		5~6
43	1833	5.27	136.6	35.5	6.4	F		
44	1854	7.9	136.0	34.75	6.9	K	25	5
45	1854	12.23	137.8	34.0	8.4	P	200	5
46	1854	12.24	135.0	33.0	8.4	P	190	5
47	1858	4.9	136.3	36.2	6.9	F		
48	1889	5.12	136.8	35.4	6.2	F		
49	1891	10.28	136.6	35.6	7.9	F		
50	1898	11.13	137.0	35.3	6.0	F		
51	1899	3.7	136.0	34.2	7.1	K	120	4
52	1900	3.22	136.2	36.0	6.1	F		
53	1901	1.16	133.7	35.3	6.1	T		
54	1903	7.6	136.6	35.0	6.2	K		
55	1906	5.5	135.4	33.8	7.1	W		
56	1909	8.14	136.3	35.4	6.4	K	45	5
57	1911	2.18	136.3	35.3	6.0	K		
58	1925	5.23	134.8	35.7	6.5	T	115	4
59	1927	3.7	135.1	35.6	7.5	T	100	5
60	1930	10.17	136.25	36.5	6.4	F		
61	1936	2.21	135.7	34.5	6.4	K	45	5
62	1938	1.12	135.2	33.7	7.2	W	160	4
63	1943	3.4	134.2	35.6	6.1	T		
64	1943	9.10	134.2	35.5	7.3	T	160	4
65	1944	12.7	136.2	33.7	8.3	P	160	4~5
66	1946	12.21	135.7	33.0	8.1	P	200	4~5
67	1948	6.28	136.3	36.1	7.2	F	120	4
68	1949	1.20	134.6	35.6	6.5	T		
69	1950	4.26	135.8	33.8	6.7	W		
70	1952	3.7	136.2	36.4	6.8	F		
71	1952	7.18	135.8	34.7	7.0	K	70	4
72	1961	8.19	136.5	36.0	7.0	F	70	4
73	1963	3.27	135.7	35.7	6.9	T		
74	1972	8.31	136.7	35.7	6.0	F		

Appendix B. Table B1. Sample Values for Duration of Stages I~IV

	Year of huge off-shore earthquakes	t_r	t_4	t_1	t_2	t_3	t_1+t_2	$\frac{t_2}{t_1+t_2}$
1	887	209.31	2.87	45.02	104.54	56.88	149.56	0.699
2	1096 1099	262.43	0.0	79.75	104.25	42.43	220.00	0.637
3	1361	137.43	9.10	79.66	0.0	48.37	79.66	0.0
4	1498	106.37	13.00	68.43	0.0	24.94	68.43	0.0
5	1605	102.73	0.0	58.36	0.0	44.37	58.36	0.0
6	1707	147.15	0.0	44.41	69.35	33.39	113.76	0.610
7	1854 1854	89.95	0.0	45.20	0.0	44.75	45.20	0.0
8	1944 1946	—	6.19	—	—	—	—	—
sum	—	—	31.16*	420.83	314.14	295.13	—	—
sample mean	—	—	7.79*	60.12	104.71	42.16	—	—
standard deviation	—	—	3.73*	14.82	28.95	9.56	—	—

(* conditional on $t_4>0$)

Appendix C. Table C1(a). Parameters for Probabilistic Model of Maximum Acceleration in Kyoto (Case 5; observed from Jan. 1979)

t (years)	n_s	n_{s1}	μ_1 (gal)	σ_1 (gal)	p_0	x_m (gal)	ζ	u_n (gal)	α_n
5	2000	138	166.15	103.31	0.93100	141.68	0.5704	119.70	0.01214
10	2000	307	173.79	95.52	0.84650	151.47	0.5347	130.59	0.01319
20	2000	767	190.03	109.28	0.61650	162.93	0.5660	140.72	0.01164
30	2000	1156	206.64	117.53	0.42200	178.24	0.5530	153.83	0.01089
40	2000	1453	217.88	117.39	0.27350	189.03	0.5488	164.92	0.01086
50	2000	1678	237.85	122.50	0.16100	208.14	0.5325	182.53	0.01041
75	1000	1000	277.77	133.48	0.0	250.07	0.4647	217.89	0.00959
100	1000	1000	304.53	132.51	0.0	279.26	0.4196	244.95	0.00964
150	1000	1000	346.79	126.49	0.0	326.81	0.3410	289.77	0.01008
200	1000	1000	383.25	136.45	0.0	362.22	0.3311	321.76	0.00934

Table C1(b). Parameters for Probabilistic Model of Maximum Velocity in Kyoto (Case 5; observed from Jan. 1979)

t (years)	n_s	n_{s1}	μ_1 (kine)	σ_1 (kine)	p_0	x_m (kine)	ζ	u_n (kine)	α_n
5	2000	138	13.37	11.83	0.93100	9.890	0.7982	8.215	0.10932
10	2000	307	13.73	11.47	0.84650	10.585	0.7314	8.772	0.11489
20	2000	767	15.51	12.67	0.61650	11.601	0.7898	9.908	0.10248
30	2000	1156	17.42	13.91	0.42200	13.230	0.7651	11.264	0.09344
40	2000	1453	18.78	14.29	0.27350	14.396	0.7647	12.434	0.09068
50	2000	1678	21.47	15.95	0.16100	16.616	0.7493	14.373	0.08113
75	1000	1000	27.00	20.50	0.0	21.850	0.6605	18.325	0.06621
100	1000	1000	30.57	19.47	0.0	25.946	0.5799	22.069	0.06676
150	1000	1000	36.55	19.89	0.0	32.569	0.4728	27.853	0.06605
200	1000	1000	41.12	21.52	0.0	37.031	0.4436	31.667	0.06080

Table C1(c). Parameters for Probabilistic Model of Maximum Acceleration in Osaka (Case 5; observed from Jan. 1979)

t (years)	n_s	n_{s1}	μ_1 (gal)	σ_1 (gal)	p_0	x_m (gal)	ζ	u_n (gal)	n
5	2000	138	152.12	88.76	0.93100	130.14	0.5791	111.61	0.01392
10	2000	307	152.66	90.99	0.84650	130.45	0.5666	111.60	0.01388
20	2000	767	177.66	108.90	0.61650	151.28	0.5674	128.89	0.01177
30	2000	1156	186.90	101.37	0.42200	162.57	0.5392	141.19	0.01258
40	2000	1453	200.65	115.26	0.27350	173.60	0.5459	149.45	0.01124
50	2000	1678	219.99	114.64	0.16100	192.77	0.5285	168.29	0.01113
75	1000	1000	257.08	127.98	0.0	230.74	0.4675	199.98	0.01006
100	1000	1000	282.47	128.60	0.0	258.13	0.4230	224.78	0.00996
150	1000	1000	324.41	122.90	0.0	304.90	0.3461	269.18	0.01040
200	1000	1000	350.91	132.66	0.0	331.23	0.3272	291.98	0.00975

Table C1(d). Parameters for Probabilistic Model of Maximum Velocity in Osaka (Case 5; observed from Jan. 1979)

t (years)	n_s	n_{s1}	μ_1 (kine)	σ_1 (kine)	p_0	x_m (kine)	ζ	u_n (kine)	α_n
5	2000	138	12.49	9.86	0.93100	9.331	0.8137	8.028	0.12636
10	2000	307	12.97	11.15	0.84650	9.486	0.8133	8.044	0.11571
20	2000	767	15.19	12.49	0.61650	11.294	0.7828	9.499	0.10086
30	2000	1156	16.19	12.36	0.42200	12.447	0.7553	10.701	0.10466
40	2000	1453	18.03	15.07	0.27350	13.678	0.7661	11.537	0.08856
50	2000	1678	20.67	15.69	0.16100	16.013	0.7459	13.751	0.08322
75	1000	1000	26.11	18.95	0.0	21.102	0.6625	17.789	0.06901
100	1000	1000	29.07	19.00	0.0	24.502	0.5864	20.713	0.06871
150	1000	1000	35.50	19.58	0.0	31.397	0.4905	26.827	0.06620
200	1000	1000	39.32	22.93	0.0	35.342	0.4353	29.859	0.0607